Mean Lifetime of the Neutral Pion

R. G. GLASSER, N. SEEMAN, AND B. STILLER
Nucleonics Division, Naval Research Laboratory, Washington, D. C.
(Received March 30, 1961)

An estimate of the mean lifetime of the π^0 meson has been obtained from an experiment employing a direct time-of-flight technique first attempted by Harris *et al.* in 1957. This method is based upon the observation in nuclear emulsion of the decay of the $K_{\pi 2}{}^+$ meson ($K^+ \rightarrow \pi^+ + \pi^0$) and the subsequent decay of the π^0 via the Dalitz mode, $\pi^0 \rightarrow e^+ + e^- + \gamma$. In the present experiment we were able to utilize a new fine-grained emulsion (Ilford L.4) that yielded markedly improved resolution. The availability of the separated K^+ beam from the Bevatron at Berkeley permitted detection and measurement of 76 Dalitz decays. We obtain, for the mean lifetime of the π^0, $\tau = (1.9 \pm 0.5) \times 10^{-16}$ sec.

I. INTRODUCTION

SINCE the publication of results[1,2] conclusively showing the existence of the neutral pion, the π^0, experimental determinations of its mass[3,4] and calculations[5,6] of the branching ratio of its decay modes have been made with increasing precision by various investigators. However, until recently,[7,8] the mean life τ of the π^0 had been only poorly determined. Theoretical calculations, using perturbation theory, predicted a value of 5×10^{-17} sec.[9] A more recent calculation,[10] using low-energy γ-p scattering data and dispersion theory, gave limits of 5×10^{-19} sec $< \tau < 10^{-16}$ sec. Early measurements of τ, summarized by Anand,[11] gave limits ranging from $< 10^{-11}$ sec to $> 10^{-15}$ sec. The availability of high-energy meson beams from accelerators made it possible to measure the value of τ in various interactions producing neutral pions under controlled experimental conditions and with much better statistics. In an experiment on charge exchange of negative pions, Schein *et al.*[12] obtained a limit $\tau < 4.8 \times 10^{-15}$. Harris *et al.*,[13] using time-of-flight measurements in nuclear emulsions on neutral pions coming from the two-body decay mode of the K^+ meson, obtained an upper limit of 5×10^{-16} sec. This limit resulted from their having to use emulsion with very large grains and having only a small number of events. Alternately Primakoff has suggested[14] that τ could be evaluated by studying the inverse process to the 2γ decay mode. This process is the photoproduction of a π^0 in the Coulomb field of a nucleus.[15] A preliminary value of τ, obtained recently in such an experiment, has been reported by Tollestrup.[16]

The successful production of fine-grained L.4 emulsion in large volume, by C. Waller, of Ilford Ltd., made it possible to obtain much better spatial resolution than was possible with G.5 emulsion. The unprocessed grain diameter is 0.15 μ in comparison with 0.27 μ in G.5,[17] and the processed grain diameter with the NRL processing is 0.35 μ as against 0.70 μ.

A stack made up of 84 L.4 emulsions, 4 in.$\times$6 in., was exposed to a beam of 300-Mev/c K^+ mesons at the Berkeley Bevatron.[18] The beam intensity entering the stack was 6000 K^+ per cm^2. These mesons came to rest at a depth of approximately 3.5 cm in the stack. The stack was processed using modified NRL methods described by Shapiro.[19]

An area scan was carried out, examining all K^+ endings. The density of mesons observed coming to rest in the scanned volume was 1930 K^+ per cm^3. As pointed out by Harris *et al.*,[13] the $K_{\pi 2}$ decay mode provides a π^0 meson with a unique velocity $\beta = 0.835$. Theoretical calculation shows 1.2% of all neutral pions should decay according to the mode $\pi^0 \rightarrow \gamma + e^+ + e^-$.[5,6] In the course of examining 28 600 K^+ endings, we have observed 86 cases in which the π^0 decayed via this alternate mode. Figure 1 is a photomicrograph of one of these events. One event was observed in which the π^0 decayed via $\pi^0 \rightarrow 2e^+ + 2e^-$ (double Dalitz decay).

Cases in which the electron pair originated more than

[1] R. Bjorklund, W. E. Crandall, B. J. Moyer, and H. F. York, Phys. Rev. **77**, 213 (1950).
[2] J. Steinberger, W. K. H. Panofsky, and J. Steller, Phys. Rev. **78**, 802 (1950).
[3] W. Chinowsky and J. Steinberger, Phys. Rev. **93**, 586 (1954); Panofsky, Aamodt, and Hadley, Phys. Rev. **81**, 565 (1951).
[4] R. P. Haddock, A. Abashian, K. M. Crowe, and J. B. Czirr, Phys. Rev. Letters **3**, 478 (1959).
[5] R. H. Dalitz, Proc. Phys. Soc. (London) **A64**, 667 (1951).
[6] D. W. Joseph, Nuovo cimento **16**, 997 (1960).
[7] R. G. Glasser, N. Seeman, and B. Stiller, *Proceedings of the 1960 Annual International Conference on High-Energy Physics at Rochester* (University of Rochester, Rochester, New York, 1960), p. 30. (This is a preliminary report on the present experiment.)
[8] R. F. Blackie, A. Engler, and J. H. Mulvey, Phys. Rev. Letters **5**, 384 (1960).
[9] J. Steinberger, Phys. Rev. **76**, 1180 (1949).
[10] M. Jacob and J. Mathews, Phys. Rev. **117**, 854 (1960).
[11] B. M. Anand, Proc. Roy. Soc. (London) **A220**, 183 (1953).
[12] M. Schein, J. Fainberg, D. M. Haskin, and R. G. Glasser, Phys. Rev. **91**, 973 (1953).
[13] G. Harris, J. Orear, and S. Taylor, Phys. Rev. **106**, 327 (1957).
[14] H. Primakoff, Phys. Rev. **81**, 899 (1951).
[15] V. Glaser and R. A. Ferrell, Phys. Rev. **121**, 886 (1961).
[16] A. V. Tollestrup, S. Berman, R. Gomez, and H. Ruderman, *Proceedings of the 1960 Annual International Conference on High-Energy Physics at Rochester* (University of Rochester, Rochester, New York, 1960), p. 27. A. V. Tollestrup, *Proceedings of the Berkeley Conference on Strong Interactions* (to be published).
[17] H. Greenberg and C. Waller (private communication, 1957).
[18] G. Goldhaber, S. Goldhaber, J. Kadyk, T. F. Stubbs, D. Stork, and H. Ticho, Lawrence Radiation Laboratory Report Bev-483, 1960 (unpublished).
[19] M. M. Shapiro, *Handbuch der Physik*, edited by S. Flügge (Springer-Verlag, 1958), Vol. 45, p. 342.

5 μ from the K ending were excluded. K endings within 20 μ of either emulsion surface were also rejected, since the electrons could not reliably be distinguished from accidental crossing tracks.

Since other decay modes of the K^+ also result in Dalitz pairs, an attempt was made to separate these "contamination events" from the $K_{\pi 2}$ events. Most τ' decays had already been rejected by the scanners because of the high grain density of the π^+ track. However, since the high-energy tail of the decay spectrum reaches 52.6 Mev, 6 cases had been recorded, and these were subsequently rejected on the basis of careful grain counts. The $K_{\mu 3}$ and K_{e3} decay modes also produce a single fast charged particle resembling a fast π^+, but the energy spectra are such that it is much more difficult to eliminate these events. A few cases were eliminated on the basis of scattering and grain counting, and a correction, to be described later, was made for the remainder. 75 Dalitz decay events were measured as well as the one double Dalitz decay.

II. MEASUREMENT TECHNIQUE

The measurements were performed on a Koristka R-4 microscope modified to accommodate two precision filar micrometers. In the field of view, one then could make use of two independently translatable crosshairs, one of which was also rotatable. The rotating stage of the microscope was used to orient each event so that the π^+ from the K^+ decay was aligned along the nonrotating filar crosshair. This filar line A was then temporarily translated off the track of the π^+ so as to eliminate any possible bias in prejudging the intersection of π^+ track and K ending during the subsequent electron track alignment. The second filar crosshair B was then aligned along one of the electron tracks, and its position recorded. See Fig. 2. Filar crosshair A was then repositioned along the π^+ track and filar line B was translated to the intersection of the π^+ line (filar A) and the K track, and its position recorded again. The difference of the two micrometer readings of filar B gave the distance L as shown in Fig. 2. The measurement was made three times and the average taken. The same procedure was then repeated for the second electron. Prior to the measurement of L, the dip angles of the π and the electron tracks were recorded, as well as the projected angles of the electron tracks with respect to the π^0 direction.

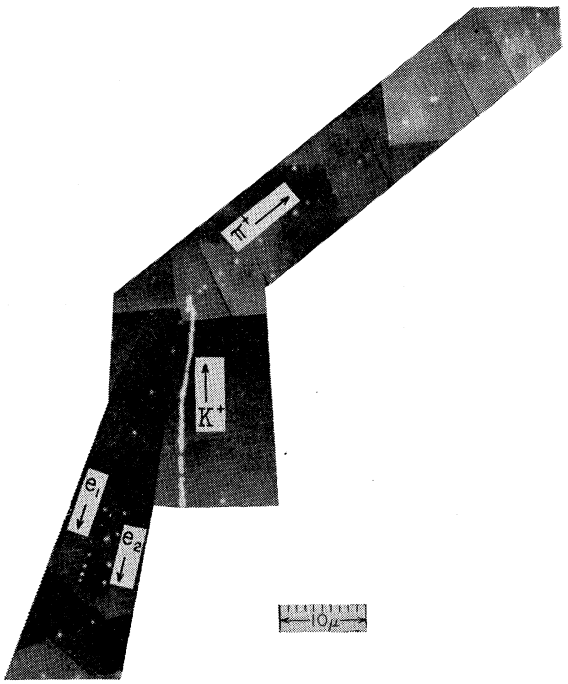

FIG. 1. Photomicrograph of a typical event used in this measurement. The K^+ meson comes to rest and decays into a π^+ and π^0 meson. The π^0, not directly observed, is emitted collinearly with the π^+ but in the opposite direction. It then decays via the "Dalitz mode," $\pi^0 \rightarrow e^+ + e^- + \gamma$. Only the electron-positron pair is observed.

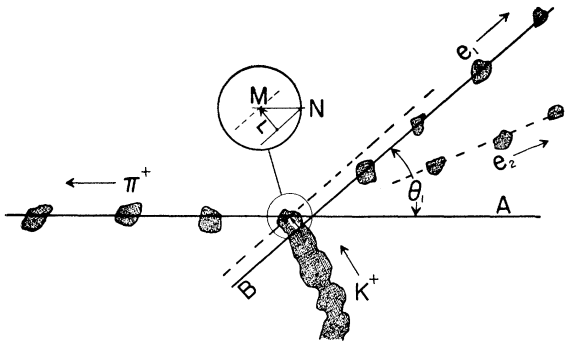

FIG. 2. Drawing to illustrate the measurement technique. A detailed explanation is given in the text. MN is the π^0 flight distance projected onto the emulsion plane. Its value is obtained from the measurement of L and θ.

These measurements were carried out at a magnification of slightly more than 1000. All the measurements used in this paper were made by one observer. The alignment procedures were restricted to the center of the field of view so that an average of five grains was employed in the alignment of a crosshair along a track. Average grain size was measured to be 0.34 μ, and the grain density (minimum) was 19 grains per 100 μ.

III. ANALYSIS OF THE DATA

The measurements just described provide a complete characterization of the geometry of the event. Since the measurements in the plane of the emulsion are much more accurate than perpendicular measurements, each event has been analyzed entirely in terms of its projection on the plane of the emulsion. At the end of the analysis of each event the mean projected distance is divided by the cosine of the pion dip angle to obtain the distance in space traversed by the neutral pion.

The fact that the $K_{\pi 2}$ is a two-body decay mode means that the line of flight of the π^+ meson is the same

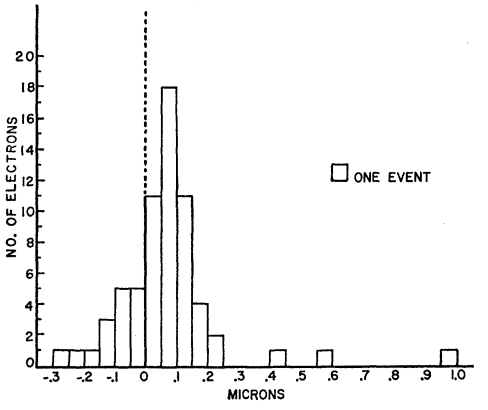

FIG. 3. Histogram of r, the π^0 flight distance projected onto the plane of the emulsion. Included in this histogram are only those events in which the electron is emitted at an angle θ with the direction of the π^0 such that $|\sin\theta| > \frac{1}{2}$.

as that of the π^0, and insures a unique velocity for the π^0. The point of origin of the π^0 is determined by using the end of the K^+ track and is required by the measurement to lie along the π^+ line. The decay point of the π^0 can be determined from the intersection of either electron with the π^+ line. This overdetermination is used to derive the precision of measurement.

If the origin of a coordinate system in the plane of the emulsion is chosen at the apparent K^+ ending, then the quantities L_1 and L_2 measured for each electron are (in magnitude) the perpendicular distances of the respective electron tracks from the origin. (See Fig. 2.) It is also convenient to choose the negative x axis to lie along the π^+ track. In the absence of error in the determination of the electron and pion lines, the electron tracks would then intersect on the x axis, that is, along the pion line of flight. The distance from their measured intersection to the x axis is used to estimate the error in determining the position of the electron

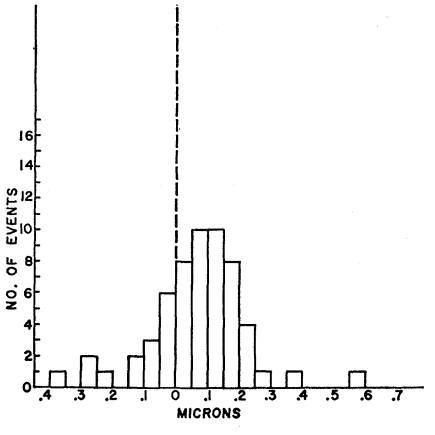

FIG. 4. Histogram of d, the π^0 flight distance. Only events for which the calculated error σ for each measurement was less than $0.20\,\mu$ have been included.

and pion lines.[20] (The mathematical details will be found in the Appendix.) It is assumed that the same error is appropriate to all these tracks, since the dominant source of error is the "grain noise" or the failure of the center of the grain (owing to its finite size) to lie precisely on the trajectory of the particle that sensitizes it. The ionization of the π^+ is slightly higher than plateau ionization, while the electrons lie somewhere between minimum and plateau ionization. Hence the difference in ionization is of the order of 10%, and this would cause a negligible difference in measurement error. The standard deviation δ, as determined from these measurements, was $0.047\,\mu$. Since we use, on the average, about 5 grains to determine the position of each track, this implies [see Appendix, Eq. (A.5)] that the error in position due to a single grain is $0.05\,\mu$ or about $\frac{1}{3}$ of the unprocessed grain diameter. This is reasonable when compared with track formation theory.

The position of the π^0 ending is determined from the intersection of each of the electron lines with the pion line. The accuracy with which this determines the position is clearly much greater when the electron track is nearly perpendicular to the pion track than when it is parallel. Those electron tracks which had an angle θ with the pion such that $\sin\theta > \frac{1}{2}$ provide most of the information. The value of r (the projected distance from the apparent K^+ ending to the π-electron intersection) is plotted for each such electron in Fig. 3.

The estimate of flight distance d for each event is found by taking a weighted mean of the two values of r obtained [see Eq. (A.11)] and dividing by the cosine of the pion dip angle. The error in d is obtained by propagating the errors of the two measurements of r and then adding the contributions from the determination of the K^+ ending [see Eq. (A.12)]. Thus for each event we obtain a value d_j of the apparent distance traveled by the neutral pion, and an error σ_j associated with the measurement. The value of σ_j, in addition to its dependence on the angles of the tracks in the event, also depends on the parameters δ already determined above and α, the standard deviation of the measurements on the K^+ ending. If it is assumed that the value of d for any given event has a statistical distribution which is the fold of the exponential decay law with a Gaussian error distribution, then the expected value of d_j is the mean decay distance λ, and the variance of d_j is $\lambda^2+\sigma_j^2$. We can now estimate α and λ by a recursion process. Assuming a value for α, we take a weighted mean and mean square of the values of d_j, using weights inversely proportional to σ_j^2. This gives an estimate of λ and of $\sum (1/\sigma_j^2)$. This last can be compared with the directly calculated value, and the value of α adjusted

[20] This estimate of precision was also used to eliminate the data of two of the three observers who attempted the measurement, since the spread of these values was much greater for these two than for the third. The difficulty in the case of one observer was traced to his inability to obtain a sharp image of the crosshair with the optical system used.

TABLE I. List of pertinent data associated with each event. See text for measurement details of r_1 and r_2, the π^0 flight distances in microns projected onto the emulsion plane. θ_1 and θ_2 are the projected angles, in degrees, between each electron and the π^0 line of flight. ϕ_1 and ϕ_2 are the electron dip angles in degrees, ϕ^0 the pion dip angle. The π^0 flight distance and its error are given, in microns, in columns labeled d and σ, respectively.

Event	r_1	r_2	θ_1	θ_2	ϕ_0	ϕ_1	ϕ_2	d	σ
45–1s	−0.23	0.24	6.8	331.4	−10.8	−13.4	46.4	0.22	0.14
45–2s	0.02	0.18	108.2	301.1	17.2	−78.8	−25.5	0.09	0.07
45–3s	0.52	1.22	354.1	355.8	−2.7	−4.1	−6.8	0.73	0.53
44–1s	0.06	0.12	332.9	333.0	13.4	13.4	−1.4	0.09	0.11
44–2s	0.00	−0.04	315.0	335.9	−52.2	−59.8	−54.1	−0.02	0.14
44–3s	0.35	0.04	25.5	29.2	10.8	29.8	33.7	0.18	0.11
44–4s	−0.07	0.23	7.5	9.1	−6.8	13.4	16.0	0.10	0.33
44–5s	0.18	0.15	333.5	349.6	33.7	−43.7	−37.4	0.21	0.17
44–6s	0.09	0.19	283.2	284.7	33.7	5.5	8.1	0.17	0.07
44–7s	0.18	−0.10	146.7	147.7	−25.5	−39.1	−39.1	0.05	0.10
44–8s	−0.02	0.08	24.8	26.4	−1.4	47.7	48.9	0.03	0.11
43–1s	0.28	0.35	352.6	354.2	−18.5	13.4	13.4	0.31	0.43
43–2s	0.12	0.09	31.9	35.7	−29.8	20.9	20.9	0.12	0.10
43–3s	1.02	0.68	4.0	7.6	43.7	−8.1	−13.4	1.02	0.61
43–4s	−1.02	2.05	356.0	359.0	31.8	−10.8	−12.1	−1.05	1.09
43–5s	0.99	0.24	46.3	50.4	−1.4	−23.2	−10.8	0.58	0.07
43–6s	−0.22	0.04	47.2	75.5	−40.7	31.8	25.5	−0.05	0.08
43–7s	−0.04	−0.01	88.2	91.4	33.7	−16.0	−18.5	−0.03	0.07
43–8s	0.12	−0.02	334.4	334.6	−16.0	42.2	42.2	0.05	0.12
41–1s	0.08	−0.11	140.5	155.3	35.6	35.6	67.3	0.04	0.11
41–2s	0.06	0.08	289.7	318.4	−63.5	83.4	78.4	0.14	0.15
41–3s	0.19	0.13	8.0	49.3	1.4	−13.4	−20.9	0.13	0.09
41–4s	0.18	0.17	20.5	24.9	35.6	−16.0	−20.9	0.21	0.15
42–1s	−0.06	−0.05	16.4	23.4	−5.5	20.9	20.9	−0.05	0.14
42–2s	0.06	0.13	123.5	124.8	−58.4	41.4	39.9	0.18	0.13
42–3s	0.59	0.30	13.2	338.8	50.6	−67.3	−70.4	0.59	0.25
42–4s	0.08	−0.69	13.7	14.2	−42.2	4.1	8.1	−0.44	0.27
42–5s	0.40	0.09	64.6	65.7	52.2	−36.5	−35.6	0.39	0.10
42–6s	0.17	0.09	24.6	37.5	31.8	−5.5	67.3	0.13	0.11
42–7s	0.05	0.01	245.5	251.1	−5.5	52.2	43.7	0.03	0.06
42–8s	−0.13	−0.05	348.2	350.0	42.2	−59.1	−59.8	−0.13	0.34
42–9s	0.10	0.05	200.7	215.8	30.8	−8.1	−57.2	0.07	0.12
42–10s	0.16	0.05	9.5	10.4	9.5	−34.7	−31.8	0.10	0.28
41–5s	0.38	0.19	345.1	346.3	−43.7	31.8	35.6	0.40	0.27
41–6s	0.02	0.11	22.9	23.7	−48.9	25.5	27.7	0.10	0.19
41–7s	0.62	0.12	346.6	347.0	27.7	−25.5	−27.7	0.42	0.24

accordingly. The values obtained are $\alpha=0.050\,\mu$ and $\lambda=0.082\,\mu$. The error calculated for this value of λ is $0.013\,\mu$. Figure 4 is a histogram of the value of d_j in the 58 events for which σ_j is less than $0.20\,\mu$.

Table I is a list of all our events with the pertinent data on each.

A somewhat more refined estimate can be made by the method of maximum likelihood. For each event we can calculate the probability density P_j that we measure the distance to be d_j:

$$P_j=\frac{1}{(2\pi)^{\frac{1}{2}}\sigma_j\lambda}\int_0^\infty \exp\left[-\frac{(d_j-s)^2}{2\sigma_j^2}-\frac{s}{\lambda}\right]ds. \qquad (1)$$

The likelihood function, $\mathfrak{L}$, is then the product of P_j for all events. The value of $\mathfrak{L}$ for the data depends on the value of λ and also on α and δ. A three-fold variation of these parameters has been carried out, computing $\mathfrak{L}$ as a function of λ, α, and δ. The values for which the curve has a maximum are $\lambda=0.082\,\mu$, $\delta=0.048\,\mu$, $\alpha=0.051\,\mu$. The close agreement between the value of δ obtained by the maximum likelihood method and the value obtained by the independent method described earlier makes one confident that no large systematic bias was present in that method. We actually used the value $0.047\ \mu$ obtained from the earlier method, since its statistical accuracy is greater. The likelihood as a function of λ for the best values of δ and α is shown as a solid line in Fig. 5. Also shown in the figure as a dashed line is the likelihood curve as a function of λ when α and δ are allowed to vary so as to obtain the maximum value of the likelihood for each λ. It is interesting to note that λ depends almost entirely on the mean value of the d_j, and α and δ on the variance. This is reflected in the fact that if quite different values are used for α and δ the estimate of λ is only slightly affected. From the shape of the likelihood curve one can estimate the standard error in the estimate of λ to be $0.16\,\mu$. The value of α from the maximum likelihood is fortuitously the same as that from the weighted mean. The estimated error is somewhat larger, and we use the larger value in the subsequent calculations.

IV. RESULTS AND DISCUSSION

The value of λ obtained in the previous section must be corrected for systematic errors. The most significant of these errors is due to the possibility of the first

TABLE I.—*Continued.*

Event	r_1	r_2	θ_1	θ_2	ϕ_0	ϕ_1	ϕ_2	d	σ
41–8*s*	−0.04	−0.07	289.0	313.9	20.9	−33.7	−18.5	−0.05	0.07
46–1*s*	0.06	0.06	66.5	66.5	−42.2	26.6	27.7	0.08	0.08
46–2*s*	0.00	0.02	118.4	122.2	66.4	−82.4	−81.8	0.02	0.16
37–1*s*	0.12	−0.34	4.4	4.5	46.4	−50.0	−51.1	−0.21	0.88
37–2*s*	−0.31	−0.40	16.9	17.0	16.0	−57.6	−50.0	−0.37	0.17
37–3*s*	0.06	0.06	308.9	315.8	57.6	−40.7	−46.4	0.11	0.14
37–4*s*	0.20	0.19	31.9	49.8	5.5	−20.9	27.7	0.19	0.08
36–1*s*	0.14	0.27	11.1	11.4	50.0	−51.7	−52.7	0.32	0.38
36–2*s*	−0.15	−0.05	291.0	307.6	23.2	−53.2	−59.1	−0.12	0.07
36–3*s*	0.39	0.01	27.4	52.7	−1.4	47.7	37.4	0.09	0.08
35–1*s*	0.00	−0.14	318.7	319.3	48.9	−27.7	−31.8	−0.10	0.12
35–2*s*	0.10	0.00	339.3	339.8	−16.0	31.8	25.5	0.05	0.14
33–1*s*	−0.17	0.22	8.9	14.2	−69.5	51.1	46.4	0.30	0.66
47–1*s*	0.17	0.15	341.9	342.2	−25.5	53.2	51.1	0.17	0.17
47–2*s*	−0.17	−0.08	29.1	35.1	56.8	−4.1	−8.1	−0.21	0.17
47–3*s*	0.14	0.11	315.1	332.0	−13.4	6.8	36.5	0.14	0.09
47–4*s*	−0.07	−0.07	28.8	33.2	18.5	5.5	4.1	−0.07	0.10
47–6*s*	0.07	0.07	131.8	138.6	−16.0	−20.9	−8.1	0.07	0.08
47–7*s*	0.04	0.03	49.5	55.8	−25.5	31.8	37.4	0.04	0.08
48–1*a*	0.06	0.22	16.0	16.3	19.7	−52.7	−52.7	0.15	0.18
48–1*b*	−0.14	−0.36	341.4	344.3	19.7	16.0	25.5	−0.25	0.17
48–2*s*	0.13	0.04	36.8	57.6	57.6	−25.5	−37.4	0.13	0.13
48–3*s*	0.24	0.32	346.9	350.2	−16.0	10.8	−1.4	0.27	0.25
48–4*s*	0.20	0.41	5.2	8.8	−35.6	−10.8	−13.4	0.42	0.46
48–5*s*	0.13	0.14	271.4	290.0	40.7	−40.7	−10.8	0.18	0.08
48–6*s*	−0.08	−0.30	27.4	325.8	40.7	−35.6	−13.4	−0.28	0.13
48–7*s*	0.03	0.27	17.7	330.2	29.8	−35.6	20.9	0.24	0.14
39–1*s*	0.04	−0.07	319.8	321.4	40.7	−33.7	−35.6	−0.02	0.11
39–2*s*	−0.01	0.16	316.0	340.7	37.4	53.2	60.5	0.02	0.11
39–3*s*	0.27	0.13	21.1	43.9	53.2	64.0	61.8	0.26	0.15
33–2*s*	0.00	−0.61	0.0	355.8	47.7	−45.1	−46.4	−0.94	1.34
33–3*s*	0.03	0.05	339.9	340.0	−16.0	20.9	20.9	0.04	0.15
33–4*s*	0.02	0.06	23.3	26.9	20.9	−8.1	−5.5	0.05	0.12
33–5*s*	1.05	0.12	4.4	60.9	27.7	9.5	19.7	0.14	0.09
49–1*s*	0.00	0.06	25.7	26.9	33.7	−8.1	−8.1	0.04	0.13
49–2*s*	0.08	0.07	41.8	43.0	59.1	−61.1	−61.1	0.14	0.15
49–3*s*	−0.06	0.00	28.2	29.3	−31.8	42.2	39.1	−0.03	0.12
49–4*s*	0.27	0.24	7.5	8.4	−35.6	35.6	35.6	0.31	0.42
49–5*s*	−0.36	0.14	4.3	36.0	−27.7	8.1	20.9	0.15	0.13
49–6*s*	−0.19	−1.83	343.9	354.4	33.7	−23.2	−20.9	−0.45	0.27
41–9*s*	0.00	−0.03	91.4	223.7	−33.7	−72.4	6.8	−0.01	0.08

grain on the π^+ track occurring so close to the K^+ ending that it merges with it. From the grain density of the π^+ tracks and the grain size, we estimate that this effect should occur in 7% of the events and lead to an average increase in d of 0.085 μ when it does occur. The net systematic error is then 0.005 μ, with an estimated uncertainty of about 50%. The direction of this effect is such as to increase the measured lifetime, but its magnitude is small enough so that it is not a serious problem.

The other decay modes of the K^+ must be considered. Fortunately the most frequent of these, the $K_{\mu 2}$, does not involve a π^0 or a γ ray and thus will not lead to a Dalitz pair. The τ mode likewise is readily distinguishable. The τ' mode, $K^+ \rightarrow \pi^+ + \pi^0 + \pi^0$, is a possible source of contamination. However, the charged secondary in every such case would have a grain density which allowed the rejection of these events as discussed in Sec. I. The $K_{\mu 3}$ and K_{e3} modes can also occur with a Dalitz pair. The frequency of these modes[21] indicates that about $\frac{1}{4}$ of our events should be from one or the other of these modes. The decays are three-body so that the velocity of the π^0 is not unique. The average velocity of the π^0, and hence the mean distance, would be lower than for a π^0 from $K_{\pi 2}$ decay. The fact that the decay is not two-body would also invalidate the geometrical assumptions for these events. The effect of including such spurious events should be to include a sample of events with lower mean apparent displacement but larger spread. The net error due to this is estimated to be of the order of 14% with an uncertainty of the same order.

The error from real γ rays converting in the vicinity can be neglected. The mean free path for pair conversion in nuclear emulsion is 3.7 cm so the probability of a γ ray converting within 5 μ is 2.7×10^{-4} or 2.3% of the probability of internal conversion; thus we should see approximately two. Actually one pair was found at about 5 μ separation and rejected.

The value of λ, taking into account the above effects, is estimated to be (0.088 ± 0.024) μ. From this the mean

[21] G. A. Snow and M. M. Shapiro, Revs. Modern Phys. **33**, 231 (1961).

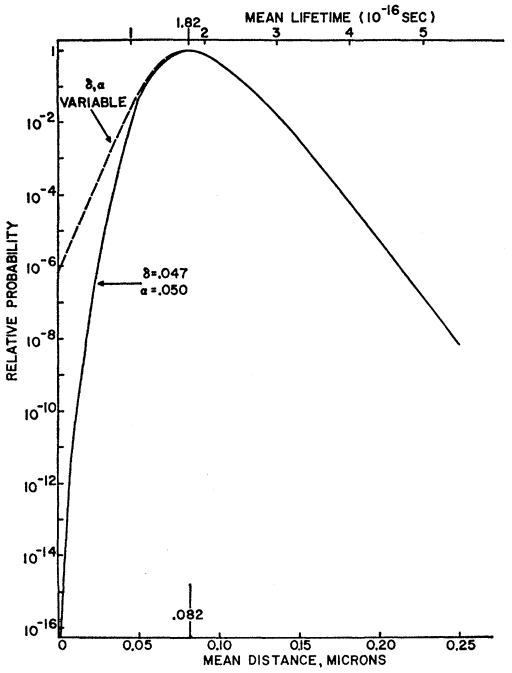

FIG. 5. Maximum likelihood curve for all of our data. The solid curve is a plot of the mean decay distance λ for the best values of the error parameters δ and α. The ordinate is a scale of relative probability. The maximum occurs at a value of $\lambda=0.082\,\mu$ corresponding to a mean lifetime of 1.82×10^{-16} sec. The dotted curve is a plot of the maximum value of the likelihood function for each λ when δ and α are allowed to vary. A scale of values of τ is included for convenience.

lifetime is estimated to be

$$\tau_{\pi^0}=(1.9\pm0.5)\times10^{-16}\text{ sec.}$$

Various checks were made to look for other possible sources of error. Identical measurements were made on twenty τ decay events. Two of the decay pions were chosen to simulate the electron pair. The same analysis as described in Sec. III was performed. The mean value of d obtained was $(-0.010\pm0.020)\,\mu$. While this gives confidence that some unknown biases were not present, it should be noted that the grain densities and multiple scattering of the tracks involved in the τ decay are different from those involved in the $K_{\pi2}$, accompanied by a Dalitz pair. The angular configurations are also very different. A small fraction of the $K_{\pi2}$ events were remeasured over an extended period of time. The results were in very good agreement with the original measurements.

In an attempt to locate possible angle-dependent biases, subdivisions of the data based on the angles of the electron tracks with respect to the pion tracks and on the dip of the electrons were made. No significant difference was found. The value of the π^0 lifetime, $(1.9\pm0.5)\times10^{-16}$ sec, obtained in this experiment is in satisfactory agreement with the value $(3.2\pm1)\times10^{-16}$ sec obtained by Blackie *et al.*[8] It is also in agreement with the value of $(1.7\pm1.4)\times10^{-16}$ sec obtained by Tollestrup *et al.*[16]

ACKNOWLEDGMENTS

The success of this experiment was dependent on the cooperation of too many people to list them all here. Particular thanks are due to our able scanning staff at NRL, Mrs. J. Leek, Mrs. Ann Bobo, and Mr. E. Lee. We also wish to acknowledge the enthusiastic assistance of Signorine A. Banfi, A. Sala, and M. Pauli, members of the scanning team of the High-Energy Physics Group, University of Milan, Italy. Mr. L. Hartman modified our Koristka R-4 microscope to allow the insertion of the second crosshair. One of us (B.S.) is also indebted to Professor G. P. S. Occhialini for his gracious invitation to work with his group at the University of Milan, and to Professor A. Bonetti for his kind hospitality during his stay there. We thank Professor E. Lofgren for making available to us the resources of the Lawrence Radiation Laboratory including the separated K^+ beam of the Bevatron. We also wish to thank Dr. M. M. Shapiro for his enthusiastic support and constructive criticism during the progress of the experiment.

APPENDIX

A. Fitting a Line

The errors involved in fitting a line to a set of grains will be discussed in terms of a least-squares fitting. In the measurements described in this paper, the line was actually fitted to the grains by setting a crosshair to pass through them. Thus the description of the errors here will apply only approximately, but it should give a sufficiently good idea of the errors for subsequent use.

A line may be described in a plane by an equation of the form:

$$f(x,y)=y\cos\theta-x\sin\theta+L=0. \qquad (A.1)$$

In this equation, θ is the angle between the positive x axis and the line, while the magnitude of L is the distance from the origin to the line. The sign of L is positive if the origin lies to the left of a vector in the direction θ in the line, and negative if to the right. The left side of the equation, $f(x,y)$, represents, for an arbitrary point (x,y) in the plane, the distance of the point from the line, with the same sign convention as described for L.

From a set of measured coordinates x_i, y_i, the least-squares condition is that

$$M=\sum_{i=1}^{n}[f(x_i,y_i)]^2 \qquad (A.2)$$

be a minimum with respect to choice of L and θ. The so-

lution to this problem is

$$\tilde{\theta}=\tfrac{1}{2}\tan^{-1}\left\{\frac{2\sum_{i=1}^{n}x_iy_i-\frac{2}{n}(\sum_{i=1}^{n}x_i)(\sum_{i=1}^{n}y_i)}{\sum_{i=1}^{n}(x_i^2-y_i^2)-\frac{1}{n}(\sum_{i=1}^{n}x_i)^2+\frac{1}{n}(\sum_{i=1}^{n}y_i)^2}\right\}. \tag{A.3}$$

$$\tilde{L}=\frac{\sin\tilde{\theta}}{n}\sum_{i=1}^{n}x_i-\frac{\cos\tilde{\theta}}{n}\sum_{i=1}^{n}y_i.$$

If the standard deviation of each coordinate measurement is represented by ϵ, then we can represent the standard error of each of the line parameters as

$$\begin{aligned}\delta\tilde{\theta}&=(12/n)^{\frac{1}{2}}(\epsilon/l),\\ \delta\tilde{L}&=(1+12q^2/l^2)^{\frac{1}{2}}(\epsilon/n),\end{aligned} \tag{A.4}$$

where l is the length of track used and q is the distance of the center of gravity of the set of grains used from the origin. Unless $q=0$, $\tilde{\theta}$ and $\tilde{L}$ are also correlated.

The origin can be conveniently chosen at the apparent end of the K^+ so that it will be at the end of the segment of track available for measurement, hence $q\approx l/2$. Also, since the distances involved are so short, the effect on the measurements used of angle errors is negligible. From now on, angle errors will be neglected and the position error will be used in the form

$$\delta\tilde{L}=2\epsilon/\sqrt{n}. \tag{A.5}$$

The measurement of grain noise as it affects multiple scattering led to an estimate of ϵ (for G.5 emulsion) of approximately 0.10 μ. This would lead to an estimate of $\delta\tilde{L}$ of 0.06 μ, about $1\frac{1}{2}$ times as large as the estimate arrived at in our measurements (in L.4 emulsion).

B. Intersections of Lines

For two lines given in the form (A.1) with parameters θ_1, L_1, and θ_2, L_2, the intersection occurs at the point

$$\begin{aligned}x&=[L_1\cos\theta_2-L_2\cos\theta_1]/\sin(\theta_1-\theta_2),\\ y&=[L_1\sin\theta_2-L_2\sin\theta_1]/\sin(\theta_1-\theta_2).\end{aligned} \tag{A.6}$$

The distance of this point from a third line with θ_0, L_0 as parameters is given by

$$p=f_0(x,y)=L_0+L_1\frac{\sin(\theta_2-\theta_0)}{\sin(\theta_1-\theta_2)}-L_2\frac{\sin(\theta_1-\theta_0)}{\sin(\theta_1-\theta_2)}. \tag{A.7}$$

If lines 1 and 2 are the measured electron tracks and line 0 is the measured pion line, then the expected value of p is 0 and its variance is (assuming all three lines have variance δ^2 associated with the measurement of L)

$$\rho^2=\delta^2\left[1+\frac{\sin^2(\theta_2-\theta_0)+\sin^2(\theta_1-\theta_0)}{\sin^2(\theta_1-\theta_2)}\right]. \tag{A.8}$$

This was used, as described in Sec. IV, to estimate the value of δ. The value obtained, 0.047 μ, is somewhat lower than the estimate made above for G.5 emulsion, presumably reflecting the smaller grain size of L.4.

For estimating the distance traveled by the neutral pion, the estimate of the pion ending is made from the intersection of the pion line and one of the electrons. The formulas simplify somewhat if we choose a coordinate system with the origin at the measured K^+ ending and the measured line of the π^+ along the negative x axis. Then from (A.6) using electron 1, we have for the measured flight distance (projected on the plane of the emulsion):

$$r_1=L_1/\sin\theta_1, \tag{A.9}$$

and similarly for electron 2. The variance of this position measurement is then

$$\delta^2(1+\cos^2\theta_1)/\sin^2\theta_1. \tag{A.10}$$

To combine the two measurements we use a weight inversely proportional to the variance:

$$r=w_1r_1+w_2r_2. \tag{A.11}$$

The variance of this combined measurement is

$$\delta^2\left[\frac{(1+\cos^2\theta_1)(1+\cos^2\theta_2)}{\sin^2\theta_1(1+\cos^2\theta_2)+\sin^2\theta_2(1+\cos^2\theta_1)}\right].$$

To this we must add the variance α^2 due to the error in the determination of the K^+ ending, giving the variance of r:

$$\alpha^2+\delta^2\frac{(1+\cos^2\theta_1)(1+\cos^2\theta_2)}{\sin^2\theta_1(1+\cos^2\theta_2)+\sin^2\theta_2(1+\cos^2\theta_1)}. \tag{A.12}$$

FIG. 1. Photomicrograph of a typical event used in this measurement. The K^+ meson comes to rest and decays into a π^+ and π^0 meson. The π^0, not directly observed, is emitted collinearly with the π^+ but in the opposite direction. It then decays via the "Dalitz mode," $\pi^0 \rightarrow e^+ + e^- + \gamma$. Only the electron-positron pair is observed.